Ibn Al-Haitham Journal for Pure and Applied Sciences

Journal homepage: http://jih.uobaghdad.edu.iq/index.php/j/index

Evaluating the Optical Properties of the Schmidt Cassegrain Spider Obscuration Telescope Using Zemax Program

Alaa B. Hasan

Department of Physics, College of Education for Pure Sciences (Ibn-AL-Haitham), University of Baghdad, Baghdad,Iraq.

alaajizany@yahoo.com

Article history: Received 19 June 2022, Accepted 21 August 2022, Published in October 2022.

Doi: 10.30526/35.4.2768

Abstract

Schmidt Cassegrain spider obscuration telescope (SCT) is one of the types of observations operating with a concave mirror. It combines several lenses and mirrors working together as an optical system. The light rays fall into the tube from the main mirror and gather on another smaller mirror called a secondary mirror. Unlike the formation of Newton's telescope, no light is made from the secondary mirror out the side of the tube but is directed to the middle of the main mirror. There is an opening in the middle of the main mirror so the light beam can go out and direct the vision lens system. The secondary mirror is located in the middle of a glass slice and is installed by thin carriers. The function of this board is to correct the portrait of the significant spherical mirror and reduce this coma aberration in the system to the lowest possible score .

In this research, the efficiency of design performance was studied due to image analysis tools provided by the Zemax program. The results showe the image quality when using a variable field of view with a limit (0^o- 0.5^o) and for a variable focal depth as needed.

Keywords: telescope, spider obscuration, concave mirror, Schmidt lens, Zemax program

1. Introduction

The great human curiosity prompted him to find ways to get to know his external world, especially the world that cannot be seen with the naked eye, whether this world is very small or very far away. Therefore, the need for the invention of the telescope or the microscope arose [1]. The telescope's design has evolved with the development of existing technologies in every era. It has kept pace with the growth of spherical lenses and mirror manufacturing, whether these objects are terrestrial or celestial [2]. The telescope was classified according to its function in observing these objects into two types: a ground-based telescope and an astronomical telescope [3].

The ground telescope includes several types according to the field of use. The telescope is used in the military, industrial, scientific, touristic, and other fields. The space telescope includes various types, including fixed ones on the surface of the earth or high in orbit around the earth in the form of a satellite (such as the Hubble telescope) [4].
There is another classification of telescopes according to the electromagnetic spectrum used. Most telescopes use visible light to create images. While in fact, visible light is a very small part of the electromagnetic spectrum emitted by celestial bodies (especially stars and galaxies). Therefore, there was a need to design telescopes that work with other spectra, such as X-rays and infrared rays (such as the James Webb telescope), which need a particular thermal environment that is not found on the surface of the earth. Therefore, it was sent at the Lagrange point to obtain orbital stability from the Earth's and Sun's gravity, as well as to be away from the thermal influence of the Sun [5].
The Schmidt Cassegrain telescope (SCT) emerged over time as one of the most popular telescope designs in the world, offering major improvements over original refractor designs. Their sharp, high-contrast images make them a good choice for the intermediate to the more experienced observer [6].
SCT combines the corrector for two optical components (mirrors). These components' locations are free, giving the designer a large design space [7]. The advantage of SCT is that it is very compact, transport, and reduces chromatic aberrations .
SCT is a hybrid design with a reflective and refractive type that uses a concave parabolic mirror (objective mirror), a secondary convex mirror (sometimes an aspheric surface), and a Schmidt lens with a special design to eliminate aberration. The objective mirror has a central hole that allows light to pass through it to reach the eyepiece (or camera or detector) after it is reflected from the secondary convex mirror, as in **Figure (1)** [8]. The arrangement of the telescope components gives a very compact design with a considerable focal length and a high magnification factor. In an asymmetrical telescope, the mirrors may be tilted to avoid obscuring the primary or avoid needing a hole in the primary mirror [8].

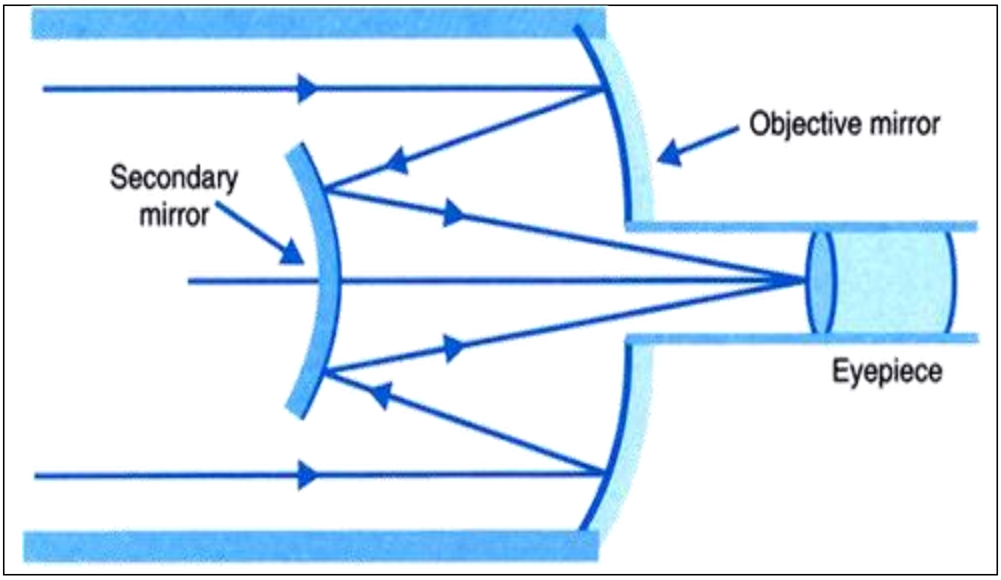

Figure 1. Internal components of SCT

The parabola shape of the primary concave mirror cancels out chromatic aberration in the image formed in the telescope. Another axial aberration is eliminated by aligning the telescope's primary and secondary mirrors on the optical axis. The design of the secondary mirror in the form of a convex hyperbola assembles the reflected rays in two foci that coincide at one point at the eyepiece lens to obtain a clear image [9].

The secondary mirror obscures the central part of the telescope aperture because it is fixed in the center. It gives an annular shape of the telescope aperture that reduces the contrast of the image due to the decrease in the value of the modified transition function (MTF) during low spatial frequencies compared to the circular aperture [10].

The radii of curvature of the primary (R1) and secondary (R2) mirrors in telescope configuration are represented by relations [11]:

$$R_1 = -\frac{2DF}{F-B} = -\frac{2F}{M} \qquad (1)$$

$$R_2 = -\frac{2DB}{F-B-D} = -\frac{2B}{M-1} \qquad (2)$$

Where F is the effective focal length of the optical system, B is the back focal length, D is the distance between two mirrors, and M is the secondary magnification.

The characteristics of telescope components are their suitability to different environmental conditions, especially temperature. The coefficient of thermal expansion is suitable for all components of the telescope to operate in a cold or hot environment. The changing temperature caused varying optical parameters of the telescope components, such as the radii curvature of the mirrors and the eyepiece lens surfaces, the refractive index of the lens, and the density of the air inside the telescope tube [12].

2. Optical Design

In this paper, the imaging system, represented by SCT, includes a cylindrical external cover of length (72 cm) and aperture diameter (24 cm). The main components of the telescope system are primary and secondary mirrors have pupil diameters (24 cm) and (8cm), respectively. The distance between two mirrors is appropriate to ensure light focuses on the image surface (eyepiece).

The telescope includes a specially designed lens called a Schmidt lens. The Schmidt lens has the feature of canceling spherical aberration through its design that changes the path of the non-axial rays so that they interact with the projections of the paraxial rays, thus canceling the aberration. The Schmidt lens is plano-convex. The plane surface faces the incoming rays at the pupil aperture. In contrast, the convex face has a curvature radius (2.5 m) to fit the telescope's dimensions and ensure the rays' refraction to the primary mirror. This prevents some rays from escaping out of the optical system.

The mirrors in SCT are a pair of mirrors for which the spherical aberration is zero, a paraboloidal primary, and a hyperboloidal secondary. The former is the perfect mirror for a point object at infinity, while the latter is perfect for finite conjugate points on opposite sides of the mirror. The conic constants of the aspherical surface of the mirror are [13]:

$$k_1 = -1 \qquad (3)$$

$$k_2 = -\frac{(m+1)^2}{(m-1)^2} \qquad (4)$$

Conic sections are important in the design of lenses and mirrors in optical imaging systems because of their geometric property that cancels out most types of aberration (axial and non-axial) that occur in the optical system. The spherical surface is characterized by the accumulation of rays in almost one point, regardless of the wide field of view, to obtain an image with suitable illumination intensity and free of aberration [14]. Thus, it is possible to overcome the aberration of non-axial rays far from the center of the optical system due to the design requirements, which need a relatively large pupil aperture to enter the largest possible amount of light rays.

The first mirror has a relatively large diameter and concave surface to collect the light coming from the source, which passes through the inner part of the telescope. The concave mirror acts as a light collector to project it onto the second mirror facing it at a distance of (32 cm) to obtain a complete collection of the reflected light from the mirror. The primary mirror is characterized by its annular shape, with an outer diameter (24 cm) and an inner diameter (8 cm). The function of the central aperture in this mirror is for light to pass through it after being reflected from the secondary mirror to reach the eyepiece.

The secondary mirror is convex with an outer diameter (8 cm) that reflects the primary mirror's light reaching the eyepiece. Its reflected surface is opposite the reflective surface of the primary mirror to change the path of the light rays in the appropriate direction. This mirror is characterized by three fixing rods in it that are fixed in the outer wall of the telescope (in the form of a spider) down to the outer frame of the secondary mirror, which is made of metal or carbon fiber according to the design. The stabilizer bars slightly affect the image quality because most of the rays from the source reach the primary mirror. The light intensity is sufficient to obtain a clear picture, as shown in Figure 2**.**

3. Imaging evaluation tools

The main function of visual optical systems is image formation. Therefore, the efficiency of any visual optical system is determined by the quality of the image formed in it. Several tools evaluate the image based on its behavior on famous mathematical functions. These functions give a clear idea of the image quality through fixed criteria for comparing the results with the ideal image [15].

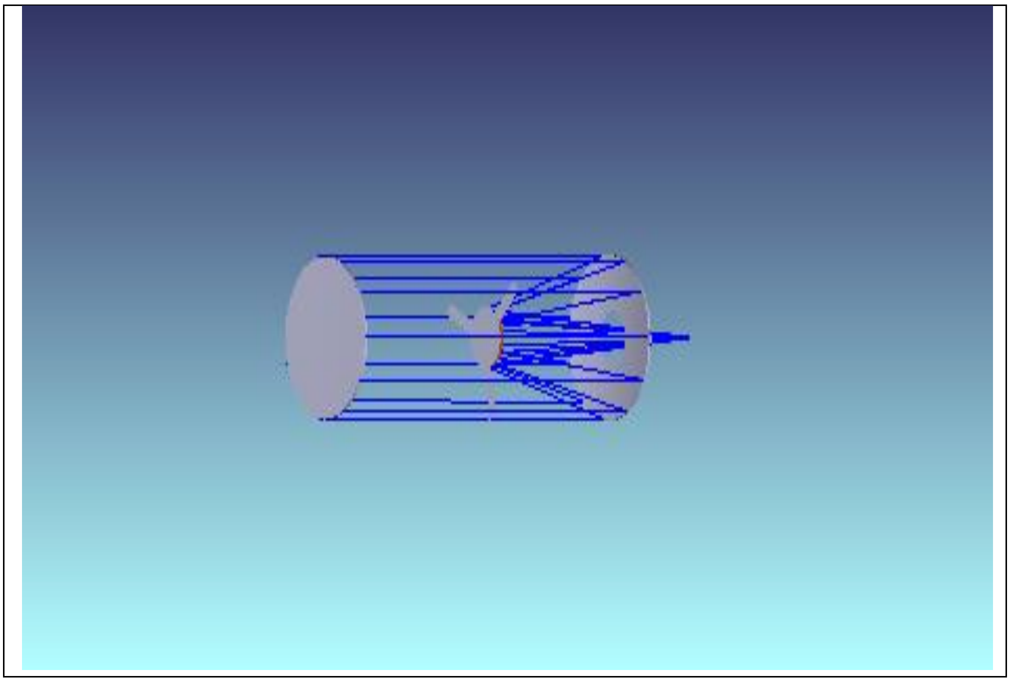

Figure 2. Layout window of SCT in Zemax Program

Zemax program provides a lot of tools that work on accurately assessing the image. Some of them depend on the macroscopic evaluation, and the other part depends on mathematical functions that work on the pattern of ray tracing through numerical mathematics or matrix representation.

The most important image evaluation tool in the Zemax program is the point spread function (PSF). This function represents the distribution pattern of light rays in the image plane of a point source. An ideal optical system would be a spot image of the point source. This spot is assembled in the center of the image where most of the rays gather there, and the intensity of the rays gradually decreases as it move away from the center, to form a special pattern called the Airy pattern, which represents a standard for the ideal image of a point object.

The other tool is the ray fan aberration curve, which represents the amount of spherical aberration present in the system. Spherical aberration occurs as a result of the passage of non-axial rays to the optical system, and these rays intersect at a place closer to the location of the focus, and the aberration occurs. The curve of ray aberration on the x- and y-axis of the image plane is fan shaped. The shape of the fan curve varies according to the amount of aberration present in the system. The bending of the fan off the axis increases as the aberration increases, so the curve gives an idea of the amount of aberration by a certain parameter of the aberration-free system (ideal case).

The use of the optical path difference shows the amount of aberration in the optical system as well. Therefore, this tool can also be used to assess image quality. The wave front curve changes when the wave travels from one medium to another through refraction of light, or the light bounces back to the same medium through reflection. The shape of the wave front changes in the case of non-axial rays than in the case of axial rays, causing aberration. The optical path difference curve determines the amount of change in the shape of the wave front when there is deviation from the ideal state.

The optical transfer function (OTF) represents the amount of contrast of the image in relation to the spatial frequency of the light entering the system. The function is at its highest value at low frequencies, so the value of the function gradually decreases when the spatial frequency increases. The amount of change in this function is calculated through a fixed standard for the ideal system. Any change in the value of the function gives an idea of the change in the quality of the image. It is preferable to use the modified optical transfer function (MTF) with a maximum value equal to one, if the medium surrounding the optical system is homogeneous.

4. Results

When observing a white light source, the effect of the dispersion phenomenon that occurs in the lenses should be calculated. The Schmidt lens has the advantage of eliminating spherical aberration, while it does not cancel out chromatic aberration, and this is clearly noticed in **Figure (3)** which shows the point spread function in the x-axis of the image plane when the source wavelength changes. The figure shows the difference in the intensity distribution in the image plane for different values of wavelength. The middle wavelengths with central peaks are the largest compared to the rest of the upper and lower wavelengths. The reason for this behavior is due to the presence of the Schmidt lens, which causes the dispersion according to wavelength.

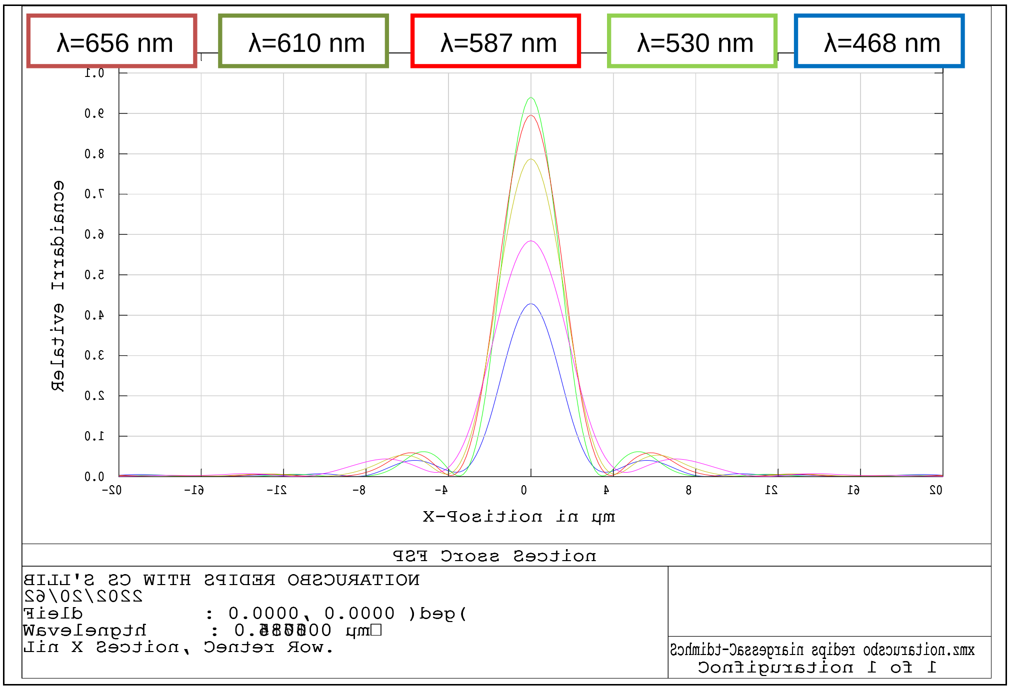

Figure 3.PSF cross section of image surface for variable wavelength in SCT

Changing the angle of the telescope's field of view affects the image quality because the off-axis object has non-axial aberration that changes the distribution of the rays' propagation in the image plane. Therefore, the object must be aligned with the telescope's optical axis to ensure a good image. **Figure (4)** shows the PSF in the image plane when the field of view angle is changed by (0^o, 0.1^o, 0.2^o, 0.3^o, 0.4^o, 0.5^o) values. The figure shows a decrease in the intensity value of the central peak when the field of view angle increases.

Therefore the object must be aligned with the optical axis of the telescope to ensure a good image.

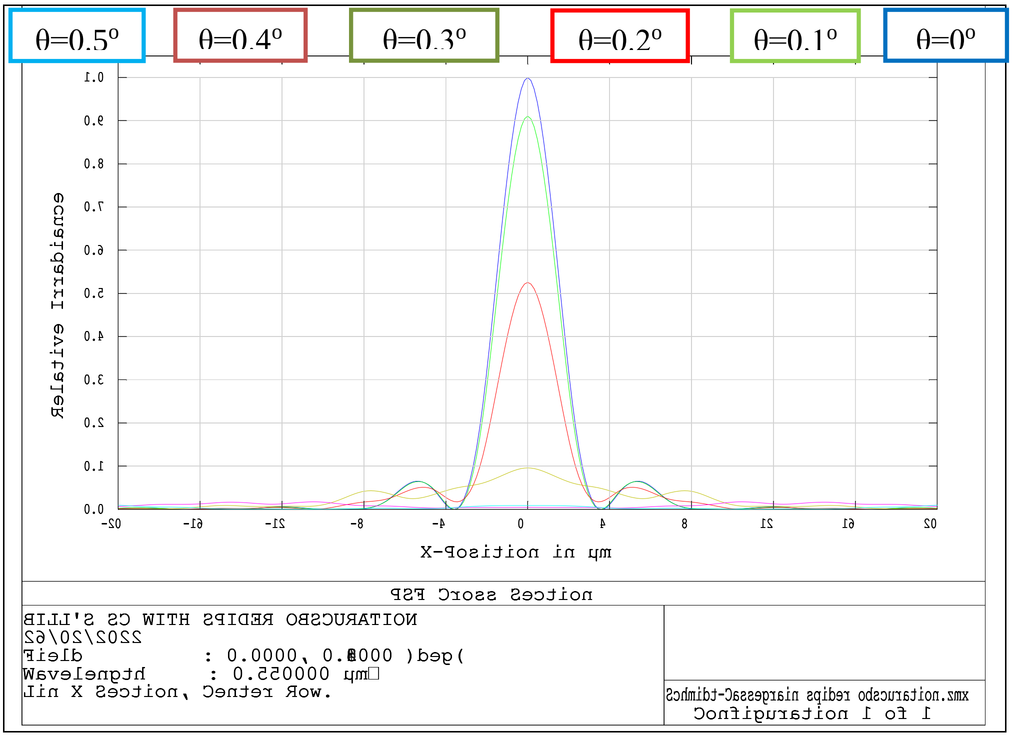

Figure 4.PSF cross section of image surface for variable field of view angle in SCT

The PSF gives an overall idea of the image quality if it is three-dimensional. The intensity distribution in the image plane can be seen more clearly in the three-dimensional plot. **Figure (5)** shows the PSF of a three-dimensional pattern in the image plane when the field of view angle changes. The figure shows an apparent change in the intensity distribution due to the field of view angle variation. Where the intensity gradually decreases with the increase of the angle due to the difference in the distribution of the optical intensity when the angle changes as a result of the increase in aberration until the intensity is absent at the angle (0.5^{o}), meaning that there are no received rays in the image plane at this angle.

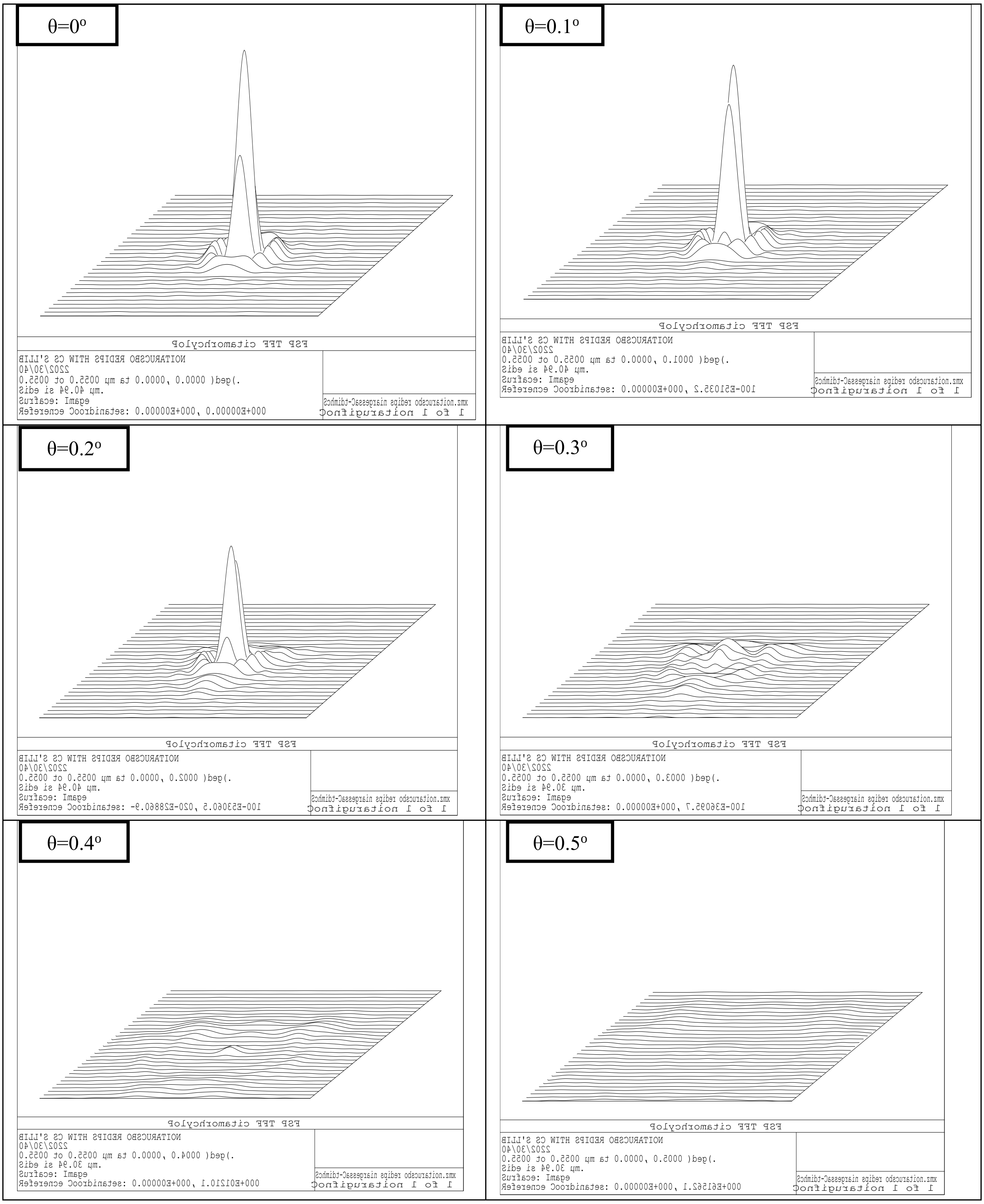

Figure 5. 3-D layout of PSF at image surface for variable field of view angle in SCT

The curve of the aberration distribution at the image plane shows the amount of deviation of the rays from their original path. When these rays are axial or non-axial, the location of their fall affects their trajectory after refraction or reflection. So, it's ideal path is according to a specific criterion. If this path changes, it indicates the presence of aberration in the optical system. The amount of aberration is determined by the amount of change of the aberration curve from the ideal path.

Figure (6) shows a diagram of the ray aberration curve of the wavelengths used when the field of view angle changes. The figure shows a gradual change in the path of the aberration curves as a result of the change in the field of view angle. This is due to changing the angle of the ray projections on the Schmidt lens and the inside of the telescope. There is also a discrepancy in the aberration curves for each wavelength due to chromatic aberration forming in the Schmidt lens.

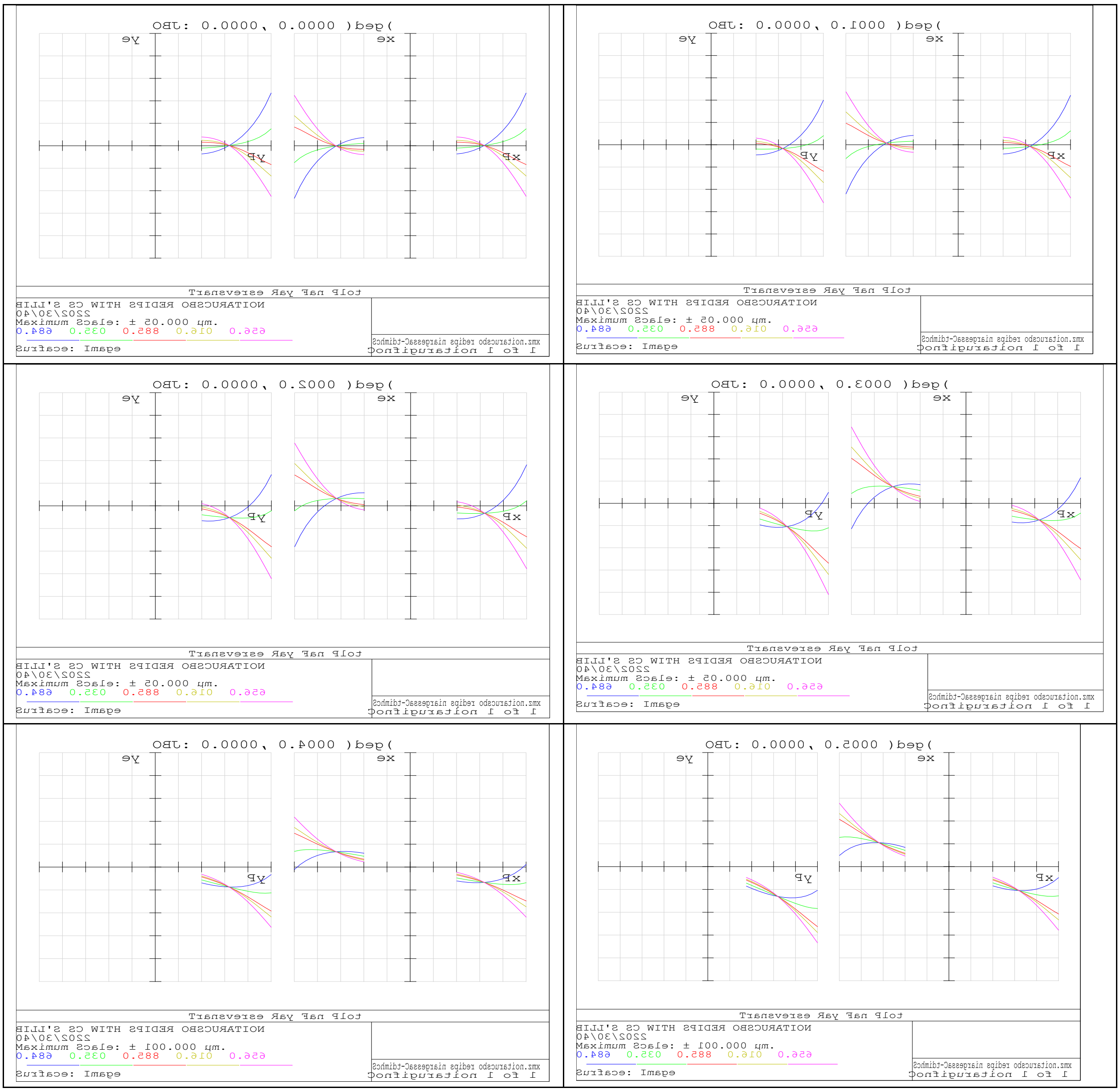

Figure 6. Ray fan aberration of multi wavelength when using different field of view angle in SCT.

The optical transfer function shows the extent of the contrast in the image when the spatial frequency of the light rays from the source changes. The value of the modified transfer function (MTF) changes from its maximum value (1) at the lowest frequency. The function drops sharply in the frequency range of less than (75 cycles/mm), after which the value of the function begins decreasing gradually until its value reaches zero.

Figure (7) shows the MTF when the field of view angle is changed for the optical system. The figure clearly shows the decrease in the value of MTF when the field of view angle is increased due to the decrease in the contrast value in the image as a result of the change in the distribution of rays propagation in the image plane.

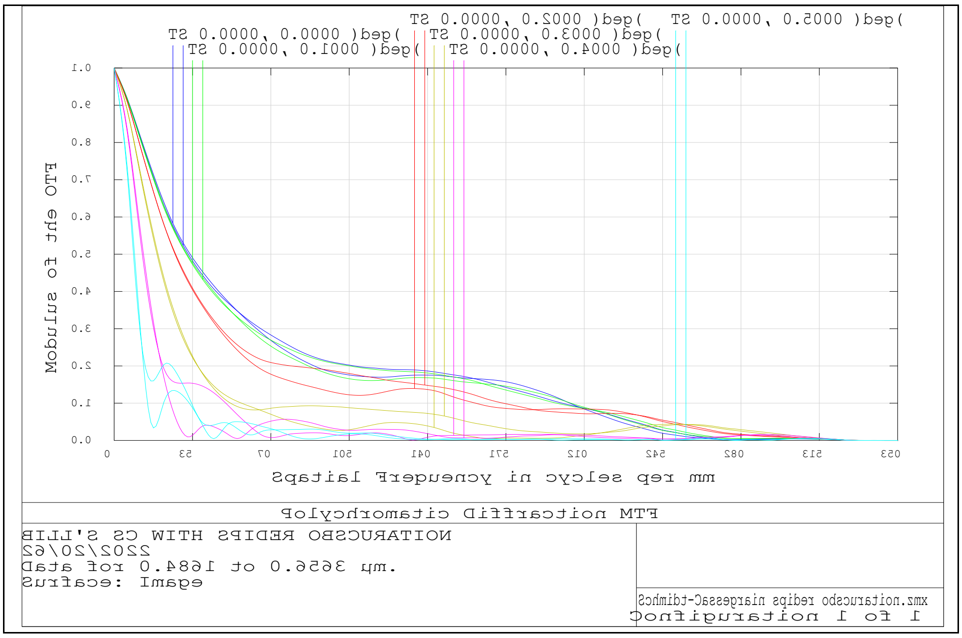

Figure 7. MTF of variable field of view angle of SCT.

5. Conclusion

The telescope's design with Schmidt lens improves the image quality by overcoming aberration. The shape of the Schmidt lens gives a special path for the rays passing through, allowing them to focus perfectly, even if the rays are far from the axis. Also, the presence of the primary and secondary mirrors in the telescope made the amount of light sufficient to obtain a good image. the study showes the importance of aligning the observed object with the telescope's optical axis due to the effect of changing the field of view angle on the image quality.

References

1. Marc, R. Zawislak.; Design Optimization Mode for a Schmidt-Cassegrain Telescope. *ME590*.Final Report, **2006**, *12*, 25-33
2. Terebizh, V. Yu. Optimal baffle design in a Cassegrain telescope. Experimental Astronomy,**2001**.*11*,171–191
3. Ivan, K.; Back to TheoryRay Tracing by Donald Feder through Aspherical Surfaces Conic Sections. *ATM Letters*,**2004**,*2*, 12-22.
4. Radziemski, L. J.; and Cremers, D. A.; Handbook of Laser Induced Breakdown Spectroscopy, *Wiley, West Sussex*, UK, **2013**. *432*. 35-44
5. De Lucia, F.; Harmon, R.;Mc-Nesby, K.;Winkel, R.; and Miziolek, A.; Laserinduced breakdown spectroscopy analysis of energetic materials, *Appl.Opt.* **2003**. 42, *30*, 6148-6152
6. Ostmark, H.; Nordberg, M.; and Carlsson, T. E.; Stand-off detection of explosives particles by multispectral imaging Raman spectroscopy, *Appl.Opt.***2011,** *50*, *28*, 5592-5599.

7. Romano, A.; and Cavaliere, R.; Newtonian and Cassegrain Telescopes, Theory and Design of Astronomical Optical Systems Using Mathematical method, *Springer International Publishing*, Cham, 2016**,** *23***,** 107-118.
8. Mullaney, J.; Reflecting Telescopes, Buyer's and User's Guide to Astronomical Telescopes & Binoculars. *Springer London*, London, **2007,***54*, 35-45
9. Schroeder, D. J.; Schmidt Telescopes and Cameras.*Astronomical Optics*, Academic Press, San Diego, **2000.** *34***.** 164-184.
10. Wilson, R. N.; Reflecting telescope optics basic design theory and its historical development. Berlin, Heidelberg, New York, *Springer*, **2007**, 234332
11. Cunningham, C.; Future optical technologies for telescopes. *Nat Photon*.**2009**, *3*.239.
12. Liu, X.; Deng, J.; Li, K.; Optical metasurfaces for designing planar Cassegrain-Schwarzschild objectives. *Phys Rev Appl*.**2019**, *11*,54-65.
13. Al-Hamdani, A.H.; Rashid, H.G.; Hasan, A.B.; Irradiance distribution of image surface in microlens array solar concentrator. *ARPN Journal of Engineering and Applied Sciences*,**2013.** *8*.10, 834–840
14. Al-Saadi, T.M.; Hussein, B.H.,; Hasan, A.B.; Shehab, A.A; Study the structural and optical properties of Cr doped SnO_2 nanoparticles synthesized by sol-gel method. *Energy Procedia*, **2019,***157*. 457–465.
15. Hasan, A.B.; Husain, S.A; Design of Light Trapping Solar Cell System by Using Zemax Program.*Journal of Physics. Conference Series.* **2018**,*1003*.1, 12-24.